Available online at www.sciencedirect.com
ScienceDirect
Pattern Recognition Letters 27 (2006) 1976–1982
Pattern Recognition Letters
www.elsevier.com/locate/patrec

Texture classification using Gabor wavelets based rotation invariant features

S. Arivazhagan [a,*], L. Ganesan [b], S. Padam Priyal [a]

[a] Department of Electronics and Communication Engineering, Mepco Schlenk Engineering College, Mepco Engineering College Post, Sivakasi 626 005, Tamilnadu, India
[b] Department of Computer Science and Engineering, Alagappa Chettiar College of Engineering and Technology, Karaikudi 630 004, India

Received 3 June 2004; received in revised form 24 December 2005
Available online 4 August 2006

Communicated by S. Ablameyko

Abstract

Texture based image analysis techniques have been widely employed in the interpretation of earth cover images obtained using remote sensing techniques, seismic trace images, medical images and in query by content in large image data bases. The development in multi-resolution analysis such as wavelet transform leads to the development of adequate tools to characterize different scales of textures effectively. But, the wavelet transform lacks in its ability to decompose input image into multiple orientations and this limits their application to rotation invariant image analysis. This paper presents a new approach for rotation invariant texture classification using Gabor wavelets. Gabor wavelets are the mathematical model of visual cortical cells of mammalian brain and using this, an image can be decomposed into multiple scales and multiple orientations. The Gabor function has been recognized as a very useful tool in texture analysis, due to its optimal localization properties in both spatial and frequency domain and found widespread use in computer vision. Texture features are found by calculating the mean and variance of the Gabor filtered image. Rotation normalization is achieved by the circular shift of the feature elements, so that all images have the same dominant direction. The texture similarity measurement of the query image and the target image in the database is computed by minimum distance criterion.

Keywords: Texture classification; Gabor wavelets; Rotation invariant features

1. Introduction

Humans are quite adaptive in dealing with textures and in the thought process, the nature of variability and patterns, edges are considered when analyzing an image. Texture refers to properties that represent the surface in reflective images and the structure of an object in transmissive images. According to Sklansky (1978), "An Image region has a constant texture if a set of local properties in that region is constant, slowly varying or approximately periodic". Texture analysis is one of the most important techniques used in the analysis and interpretation of images, consisting of repetition or quasi repetition of some fundamental image elements (e.g., Raghu and Yegnanarayana, 1996).

Analysis of texture requires the identification of proper attributes or features that differentiate the textures for classification, segmentation and recognition. Various feature extraction and classification techniques have been suggested in the past for the purpose of texture analysis. The traditional statistical approaches to texture analysis such as co-occurrence matrices, second order statistics, Gauss–Markov random fields and local linear transforms (e.g., Haralick et al., 1973; Davis et al., 1979; Chen and Pavlidis, 1983; Kashyap and Khotanzed, 1986; Chellappa and Chatterjee, 1986; Derin and Elliot, 1987; Unser, 1986) are

* Corresponding author. Tel.: +91 4562 235400; fax: +91 4562 235111.
E-mail address: s_arivu@yahoo.com (S. Arivazhagan).

0167-8655/$ - see front matter © 2006 Elsevier B.V. All rights reserved.
doi:10.1016/j.patrec.2006.05.008

restricted to the analysis of spatial interactions over relatively small neighborhoods on a single scale. As a consequence, their performance is best for the analysis of micro-textures only (e.g., Unser, 1995). Moreover, they are single resolution techniques, resulting in poor performance for texture analysis.

More recently, methods based on multi-resolution or multi-channel analysis such as *Wavelet transform* and *Gabor filters* have gained a lot of attention for texture analysis such as texture classification and texture segmentation and related applications. The use of a pyramid structured wavelet transform for texture analysis was first suggested in the pioneering work of Mallat (1989). This initial proposal has been followed by several studies on texture analysis using wavelet transform (e.g., Laine and Fan, 1993; Chang and Kuo, 1994; Unser, 1995; Wang et al., 1998; Van De Wouwer et al., 1999; Wang and Liu, 1999; Pun and Lee, 2001; Charalampidis and Kasparis, 2002; Manthalkar et al., 2003b; Arivazhagan and Ganesan, 2003). But, the wavelet transform decompose the given image in to only three directional components, i.e., horizontal, diagonal and vertical detail sub bands in the direction of 0°, 45° and 135° respectively apart from the approximation (or) smooth sub band. This limits the application of wavelet transform for rotation invariant texture analysis.

Feature extraction using Gabor functions is motivated by the fact that, these filters can be considered as orientation and scale tunable detectors. Basically, Gabor filters are a group of wavelets, with each wavelet capturing energy at a specific frequency and at a specific orientation or direction. There are several approaches to texture classification and segmentation, both supervised and unsupervised, using banks of Gabor filters with different scale and orientation tuning (e.g., Tuner, 1986; Fogel and Sagi, 1989; Bovik et al., 1992; Du Buf, 1990; Jain and Farrokhnia, 1991; Dunn and Higgins, 1995; Teuner et al., 1995; Haley and Manjunath, 1995; Pichler et al., 1996; Idrissa and Acheroy, 2002). Rotation invariant texture classification using wavelet transform is addressed in (e.g., Pun and Lee, 2001; Charalampidis and Kasparis, 2002; Manthalkar et al., 2003b), while Gabor filter based rotation invariant texture classification is discussed in (e.g., Haley and Manjunath, 1995; Manthalkar et al., 2003a). Further, Circular Gabor Filter (CGF) was used for rotation invariant texture segmentation in (e.g., Zhang and Tan, 2002) and circular Gabor based object matching was done in (e.g., Zhu et al., 2004). However, they have not used CGF for texture classification.

The objective of this paper is to achieve rotation invariant texture classification for a larger texture database of 112 textures from Brodatz album with 4032 rotated textures derived from them, by extracting Gabor wavelet based features. For feature-based approaches, rotation invariance was achieved by employing DFT based approaches as defined in (e.g., Kashyap and Khotanzed, 1986). In this paper rotation normalization method, that achieves rotation invariance by a circular shift of the feature elements so that all images have same dominant direction, is adopted. It is proved that the rotation in spatial domain is equivalent to circular shift of Gabor elements (e.g., Zhang et al., 2000). Then, a suitable distance metric is used to compare it with the features of known texture. Also, the results obtained with the proposed method are compared with the results of single and multi-channel CGFs.

This paper is organized as follows. Section 2 describes the fundamentals of Gabor functions. Section 3 discusses texture representation and classification based on the output of the Gabor filters. In Section 4 experimental results and discussion have been provided and Section 5 concludes the paper.

2. Gabor functions

2.1. One-dimensional Gabor function

A Gabor function is defined as a harmonic oscillator, which is complex sinusoidal plane wave of some frequency and orientation within a Gaussian envelope. Thus, it can be stated that Gabor function is the product of a Gaussian function and a complex sinusoid. Its general one-dimensional form is given in Eq. (1).

$$G(x) = \frac{1}{\sqrt{2\pi}\sigma} \exp\left(\frac{-x^2}{2\sigma^2}\right) \exp(j\pi Wx). \tag{1}$$

Thus, Gabor functions are bandpass filters. Gabor functions are used as complete, albeit non-orthogonal, basis sets.

2.2. Two-dimensional Gabor function

A 2-D Gabor filter is an oriented sinusoidal grating modulated by a 2-D Gaussian function, with a modulation frequency 'W', and is given in Eq. (2).

$$G(x,y) = g_\sigma(x,y)\exp(2\pi jW(x\cos\theta + y\sin\theta)), \tag{2}$$

where,

$$g_\sigma(x,y) = \left(\frac{1}{2\pi\sigma_x\sigma_y}\right)\exp\left(\frac{-1}{2}\left(\frac{x^2}{\sigma_x^2} + \frac{y^2}{\sigma_y^2}\right)\right).$$

The Gabor filtered output of an image $f(x,y)$ is obtained by the convolution of the image with the Gabor function $G(x,y)$. The parameters of a Gabor filter are the modulation frequency W, the orientation parameter θ and the scale σ of the Gaussian function. Local orientations and spatial frequencies explicit in Gabor filters are therefore used as the key features for texture processing. The input image is generally filtered by a family of Gabor filters tuned to several resolutions and orientations.

2.3. Gabor wavelet transform

The Gabor functions form a complete but non-orthogonal basis set and any given function $f(x,y)$ can be expanded in terms of these basis functions. Such an expansion provides a localized frequency description and has been used in image compression and texture analysis. Local frequency analysis however is not suitable for feature representation as it requires a fixed window width in space and consequently the frequency bandwidth is constant on a linear scale. In order to optimally detect and localize features at various scales, filters with varying support rather than a fixed one are required. This led to the implementation of a transform similar to wavelet decomposition, where the basic wavelet is a Gabor function.

A Gabor wavelet is also a complex planar wave restricted by 2-D Gaussian envelope. Aside from scale and orientation, the only thing that can make two Gabor wavelets differ is the ratio between wavelength and the width of the Gaussian envelope. Every Gabor wavelet has a certain wavelength and orientation, and is then convolved with an image to estimate the magnitude of local frequencies of that approximate wavelength and orientation in the image. The Gabor wavelets can be considered as a class of self-similar functions. Let $g(x,y)$ be the mother Gabor wavelet, then this self-similar filter set is obtained by appropriate dilations and rotations of the mother wavelet. For a given image $I(x,y)$ of size MxN, its discrete Gabor wavelet transform is given by convolution Eq. (3).

$$G_{pq}(x,y) = \sum_s \sum_t I(x-s, y-t)\psi^*_{pq}(s,t), \tag{3}$$

where s, t are the filter mask size variables; p, q are the scale and orientation values respectively and ψ^*_{pq} is the complex conjugate of ψ_{pq}, which is a self-similar function generated from the dilation and rotation of the mother wavelet 'ψ' and is defined as given in Eq. (4).

$$\psi(x,y) = \left(\frac{1}{2\pi\sigma_x\sigma_y}\right)\exp\left(\frac{-1}{2}\left(\frac{x^2}{\sigma_x^2}+\frac{y^2}{\sigma_y^2}\right)\right)\exp(2\pi jWx). \tag{4}$$

The Gabor wavelets are obtained through the generating function defined in Eq. (5).

$$\psi_{pq}(x,y) = a^{-p}\psi(\bar{x},\bar{y}), \tag{5}$$

where $p = 0,1\ldots P-1$ and $q = 0,1\ldots Q-1$; a, the scale factor; P, the total number of scales; Q, the total number of orientations; $\bar{x} = a^{-p}(x\cos\theta + y\sin\theta)$ and $\bar{y} = a^{-p}(-x\sin\theta + y\cos\theta)$, for $a > 1$ and $\theta = \frac{q\pi}{Q}$.

3. Texture representation and classification

This section describes texture representation based on Gabor transform and texture classification with rotation normalization. The purpose of texture classification is to identify similar texture images.

3.1. Texture representation

A set of Gabor wavelets of different scale and orientation is convolved with an image to estimate the magnitude of local frequencies of that approximate scale and orientation. The output obtained by applying Gabor filter on a brick texture image for 19 different orientations in steps of 10° is shown in Fig. 1.

After applying Gabor filters on the image with different orientation at different scale, the energy content is calculated using Eq. (6).

$$E(p,q) = \sum_x \sum_y |G_{pq}(x,y)|. \tag{6}$$

The mean μ_{pq} and standard deviation σ_{pq} of all transformed coefficients are found using Eqs. (7) and (8) respectively. These values represent the feature of the homogeneous texture image.

$$\mu_{pq} = \frac{E(p,q)}{MN}, \tag{7}$$

$$\sigma_{pq} = \sqrt{\frac{\sum_x\sum_y |G_{pq}(x,y)| - \mu_{pq}}{MN}}. \tag{8}$$

A feature vector 'F' for texture representation is created using the mean and standard deviation as feature components. If P scales and Q orientations are considered in the implementation, then the corresponding feature vector is given in Eq. (9).

$$F = (\mu_{00}, \sigma_{00}, \mu_{01}, \sigma_{01}, \ldots, \mu_{P-1Q-1}, \sigma_{P-1Q-1}). \tag{9}$$

3.2. Rotation invariant measurement

The texture similarity measurement between the query image (U) and the target image (T) in the database are accomplished by defining the distance metric, given in Eq. (10).

$$d_{pq}(U,T) = \sqrt{(\mu^U_{pq} - \mu^T_{pq})^2 + (\sigma^U_{pq} - \sigma^T_{pq})^2}. \tag{10}$$

For N number of images in the database the query image U is classified as belonging to target image 'T' for:

$$D(U,T) = \mathrm{Min}\left(\sum_p \sum_q d_{p,q}(U,T)\right); \quad \text{for } T = 1,2,\ldots,N. \tag{11}$$

Since this similarity measurement is not rotation invariant, similar texture images with different direction will be classified erroneously. Fig. 2(a) and (b) shows the Bark texture image in different orientations but will have very big distance if the above measurement is applied directly. Expensive calculation is involved if feature elements are shifted in all the directions to find the best match between query image and target images. Hence, a simple circular shift on the feature map is employed to solve the rotation variant problem (e.g., Zhang et al., 2000).

In this method, the total energy for each orientation is calculated using Eq. (6). The orientation with highest total energy is called the dominant orientation. The feature element in dominant orientation is moved as first element in

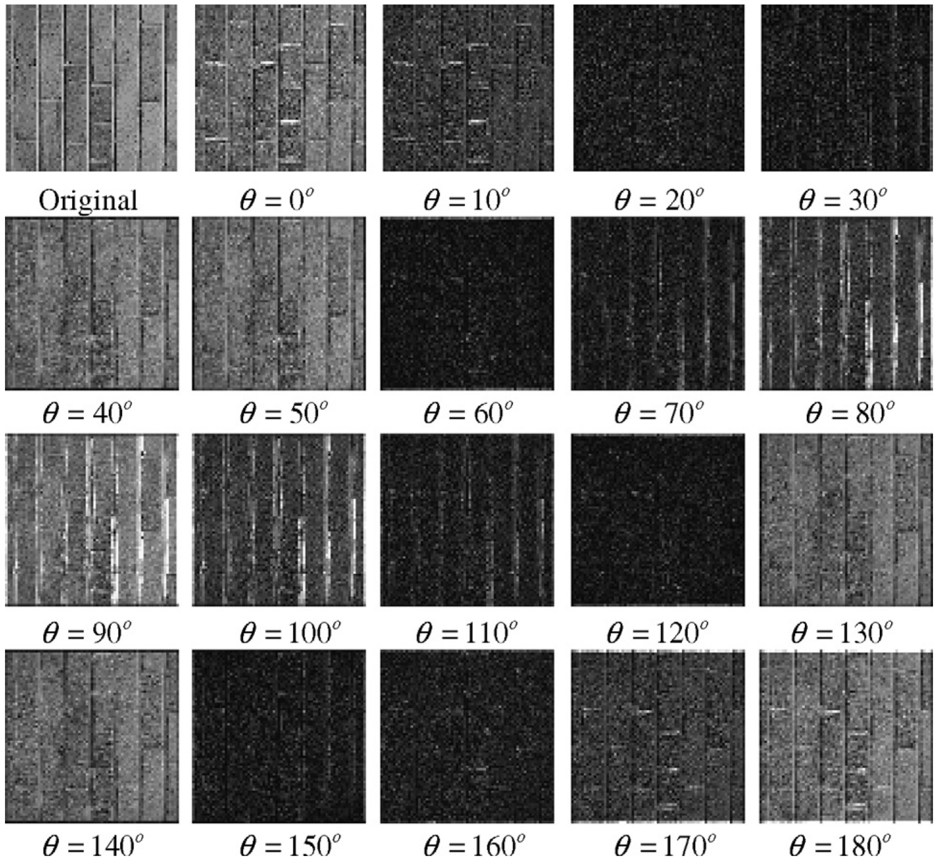

Fig. 1. Gabor transform results obtained for 19 orientations (steps: 10^0) at $scale = 2$.

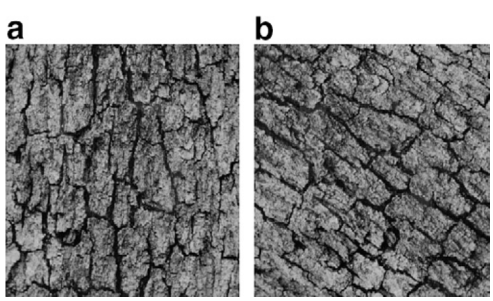

Fig. 2. Sample texture image: (a) original bark image and (b) rotated bark image.

the feature vector F. Then, the other elements are circularly shifted. For example, if the original feature vector is "*abcdef*" and "*c*" is at the dominant direction, then the normalized feature vector will be "*cdefab*". This normalization method is based on the assumption that to compare similarity between two textures, they should be rotated so that their dominant directions are the same. It has been proved that image rotation in spatial domain is equivalent to circular shift of feature vector elements (e.g., Zhang et al., 2000).

4. Experimental results and discussion

Experiments are conducted with two groups of textures, the first group consists of 13 primary textures, collected from Brodatz (1966) texture album and the second group consists of all the 112 textures of Brodatz album. In our experimentation, conducted with first group of textures the level of Gabor decomposition chosen is five and orientation is six and thus 30 Gabor filters are used. The first groups of texture images of size 512×512 at 0° used in training phase are: (i) Bark, (ii) Brick, (iii) Bubbles, (iv) Grass, (v) Leather, (vi) Pigskin, (vii) Raffia, (viii) Sand, (ix) Straw, (x) Water, (xi) Weave, (xii) Wood and (xiii) Wool. Texture classification is done with a total of 91 rotated textures of size 512×512 ($13 \times 7 = 91$) of first group of 13 textures, each at seven different orientations of 0°, 30°, 60°, 90°, 120°, 150° and 200°. The results obtained for the first group of textures are given in Table 1, where each entry corresponds to average classification rate for seven rotated textures of different orientations and a mean success rate of 95.60% is reported as shown in the Table 1. For the purpose of comparison, texture classification experiment is repeated with the same 91 rotated textures but with wavelet statistical and wavelet co-occurrence features (WSF and WCF), used in (e.g., Arivazhagan and Ganesan, 2003). The results obtained for WSFs and WCFs are also given in the same Table 1. Here, a mean success rate of only 58.24% is obtained which clearly shows the poor directional property of discrete wavelet transform.

The second group of textures, comprising all the 112 textures of size 512×512 from the Brodatz album

Table 1
Results of rotated texture classification using WSFs and WCFs and Gabor features for 13 Brodatz texture images (with 91 rotated textures)

Sl. no.	Images	Correct classification (%)	
		Feature vectors	
		WSFs and WCFs	Gabor features
1	Bark	100	100
2	Brick	100	85.71
3	Bubbles	0	100
4	Grass	100	100
5	Leather	71.43	100
6	Pigskin	42.86	100
7	Raffia	28.57	100
8	Sand	100	100
9	Straw	0	100
10	Water	100	100
11	Weave	57.14	100
12	Wood	57.14	100
13	Wool	0	57.14
Number of rotated images correctly classified		53	87
Mean success rate		58.24	95.60

(D1–D112) are used in the training phase and they are rotated in steps of 10° up to 360° and used for classification, i.e., texture classification is done with a total of 4032 rotated texture images ($112 \times 36 = 4032$) for various combination of scale and orientation values of Gabor decomposition. The rotated textures are of size 256×256, derived from the center portion of respective 512×512 size rotated textures. The consolidated results, obtained for nine different Gabor wavelet feature vectors (*F1–F9*) and for six different combinations of scale and orientation values are shown in Table 2. For the purpose of comparison, texture classification experiment is repeated with single and multi-channel circular Gabor filter (CGF) methods used in (e.g., Zhang and Tan, 2002; Zhu et al., 2004) for the same 112 Brodatz texture images and their consolidated results are also given in the Table 2. As shown in the Table 2, the consolidated results provide the number of features used, the mean success rate achieved and the minimum classification rate obtained for different feature vectors. Also, the Table 2 shows texture image(s) for which minimum classification rate is obtained for the given feature vector.

From the Table 2, it is observed that the highest mean success rate of 93.73% is obtained for *feature vector F7* (*with* 100 *features*), i.e., for Gabor wavelet decomposition (with $scale = 5$ and $orientation = 10$). The next highest mean success rate of 93.53% is obtained for *feature vector F2* (with $s = 4$ and $o = 12$ and 96 *features*). The next highest mean success rate of 93.43% is obtained for *feature vector F9* ($s = 10$ and $o = 10$), where classification is done with 200 *features*. Also, a little less mean success rate of 93.38% is obtained for *feature vector F6* ($s = 5; o = 6$) with 60 *features*. For *feature vector F5* ($s = 5; o = 6$) with *just* 30 *features* of 15 selected sub bands, a mean success rate of 92.96% is obtained which is certainly a performance, comparable to the highest mean success rate of 93.73%, obtained for *feature vector F7* (*with* 100 *features*). However, for the above *feature vector F5*, a minimum classification rate of only 11.11% is obtained for D83 and D110 textures. Further it is interesting to note that, for feature vector *F3*($s = 5; o = 6$) with only 2 features, i.e., dominant mean and variance features of 30 sub-bands of Gabor decomposed images, a mean success rate of 92.41% is obtained. Though, it is the lowest mean success rate among the nine feature vectors, it is just less than by 1.32% from the highest mean success rate (i.e., 93.73%), obtained for feature vector *F7* with 100 features. Since there is no vast difference between the mean success rates achieved for different feature vectors, the best feature vector can be decided by taking in to account the number of features used and the minimum classification rate obtained for different feature vectors. Based on this criteria, the *feature vector F6* ($s = 5; o = 6$) *with* 60 *features* and with a mean success rate of 93.38% and a minimum classification rate of 44.44% can be chosen as the best among 9 feature vectors.

Table 2
Consolidated results of rotated texture classification using Gabor wavelet features (*F1–F9*) and single and multi-channel circular Gabor filters (CGF) for 112 Brodatz texture images (with 4032 rotated texture images)

Feature vectors with different scales (s) and orientations (o) of Gabor decomposition	No. of features used	Number of rotated texture images correctly classified	Mean success rate (%)	Minimum classification rate (%) and the corresponding texture (s)
F1 – ($s = 4; o = 8$)	64	3745	92.88	33.33 – D103
F2 – ($s = 4; o = 12$)	96	3771	93.53	22.22 – D21
F3 – ($s = 5; o = 6$)	2[a]	3726	92.41	27.77 – D72
F4 – ($s = 5; o = 6$)	14[a]	3729	92.49	11.11 – D83, D110
F5 – ($s = 5; o = 6$)	30[b]	3748	92.96	11.11 – D83, D110
F6 – ($s = 5; o = 6$)	60	3765	93.38	44.44 – D62, D70, D75
F7 – ($s = 5; o = 10$)	100	3779	93.73	11.11 – D21
F8 – ($s = 10; o = 6$)	120	3758	93.20	27.77 – D78
F9 – ($s = 10; o = 10$)	200	3767	93.43	33.33 – D102
Single channel CGF	2	2736	67.86	5.55 – D11, D16, D43
Multi-channel CGF	14	3031	75.17	8.33 – D17

[a] Dominant mean and variance features.
[b] Features of 15 selected sub bands.

Further, it is found that the rotation invariant circular Gabor filter (CGF) methods used by Zhang and Tan (2002) and Zhu et al. (2004) perform poorly than the proposed method for texture classification as evident in the Table 2. Though, the average time taken for classification of an image at one orientation is comparatively less for CGF methods (i.e., 1.01 s for single channel CGF with 2 features and 1.43 s for seven channel CGF with 14 features against 3.40 and 5.31 s for the proposed method with 2 and 14 dominant features respectively), their mean success rates are poor. The single channel CGF with two features results in a mean success rate of 67.86% only against 92.41% obtained for Gabor wavelet feature vector *F3* with two features while the mean success rate of multi-channel CGF with 14 features is 75.17% against 92.49% obtained for Gabor wavelet feature vector *F4* with fourteen features. The programs were developed in MATLAB and executed in Intel Celeron @ 1.7 GHz system with 128 MB RAM.

5. Conclusion

In this implementation, experimentation is conducted with 4032 rotated textures derived from all the 112 Brodatz texture images for different Gabor wavelet decomposition parameters (scale = up to 10; orientation= up to 10), against 872 samples of 109 Brodatz texture images for Gabor wavelet decomposition parameters (scale = up to 4; orientation = up to 4) used by Haley and Manjunath (1999). The mean success rate and misclassification rate per competing texture type, obtained with their method are 80.4% and 0.18% against 93.73% and 0.06% respectively, obtained in our implementation. Further, they have used non-overlapping set of 872 samples for training and 872 samples for classification. But in our implementation, only 112 textures at 0° orientations are used in the training phase while 4032 rotated textures derived from the above 112 textures are used for classification. Also, the comparative analysis with the recently proposed rotation invariant circular Gabor filter methods used by Zhang and Tan (2002) and Zhu et al. (2004) show that CGF methods result in poor performance than the proposed method. The mean success rate obtained with multi-channel circular Gabor filter method is 75.17% only against the highest mean success rate of 93.73%, obtained in the proposed method, of course with a little time complexity.

Hence, the approach described herein has proven to be effective for rotation invariant texture classification. Though techniques based on co-occurrence matrix computation have proven effective for texture classification, the use of Gabor wavelets ensures enhanced classification results only with first order statistical features, such as mean and standard deviation. The procedure based on co-occurrence matrix is computationally expensive compared with those employing Gabor wavelet features. Further, the work can also be extended for scale invariance, defining a scale normalization procedure.

Acknowledgements

The authors are grateful to the Management and Principal of Mepco Schlenk Engineering College, Sivakasi for their constant support and encouragement. The authors also extend their gratitude to the anonymous reviewers who have given very good suggestions for this better presentation of our manuscript.

References

Arivazhagan, S., Ganesan, L., 2003. Texture classification using wavelet transform. Internat. J. Pattern Recognition Lett. 24 (9–10), 1513–1521.

Bovik, A.C., Gopal, N., Emmoth, T., Restrepo, A., 1992. Localized measurement of emergent image frequencies by Gabor wavelets. IEEE Trans. Inform. Theory 38 (2), 691–712.

Brodatz, P., 1966. Textures: A Photographic Album for Artists and Designers. Dover, Toronto.

Chang, T., Kuo, C.C.J., 1994. Texture analysis and classification with tree-structured wavelet transform. IEEE Trans. Image Process. 2 (4), 429–441.

Charalampidis, D., Kasparis, T., 2002. Wavelet-based rotational invariant roughness features for texture classification and segmentation. IEEE Trans. Image Process. 11 (8), 825–837.

Chellappa, R., Chatterjee, S., 1986. Classification of textures using Gaussian Markov random fields. IEEE Trans. Acoust. Speech, Signal Process. ASSP-33 (4), 959–963.

Chen, P.C., Pavlidis, T., 1983. Segmentation by texture using correlation. IEEE Trans. Pattern Anal. Machine Intell. PAMI-5, 64–69.

Davis, L.S., Johns, S.A., Aggarwal, J.K., 1979. Texture analysis using generalized co-occurrence matrices. IEEE Trans. Pattern Anal. Machine Intell. PAMI-1, 251–259.

Derin, H., Elliot, H., 1987. Modeling and segmentation of noisy and textured images using Gibbs random fields. IEEE Trans. Pattern Anal. Machine Intell. PAMI-9, 39–59.

Du Buf, J.M.H., 1990. Gabor phase in texture discrimination. Signal Process. 21 (3), 221–240.

Dunn, D.F., Higgins, W.E., 1995. Optimal Gabor filters for texture segmentation. IEEE Trans. Image Process. 4 (7), 947–964.

Fogel, I., Sagi, D., 1989. Gabor filters as texture discriminator. Biol. Cybern. 61, 103–113.

Haley, G.M., Manjunath, B.S., 1995. Rotation invariant texture classification using modified Gabor filters. In: Proc. IEEE Int. Conf. Image Processing, Washington, DC.

Haley, G.M., Manjunath, B.S., 1999. Rotation-invariant texture classification using a complete space-frequency model. IEEE Trans. Image Process. 4, 255–269.

Haralick, R.M., Shanmugam, K., Dinstein, I., 1973. Textural features for image classification. IEEE Trans. Systems, Man Cybernet. 3, 610–621.

Idrissa, M., Acheroy, M., 2002. Texture classification using Gabor filters. Pattern Recognition Lett. 23 (9), 1095–1102.

Jain, A.K., Farrokhnia, F., 1991. Unsupervised texture segmentation using Gabor filters. Pattern Recognition 24 (12), 1167–1186.

Kashyap, R.L., Khotanzed, A., 1986. A model based method for rotation invariant texture classification. IEEE Trans. Pattern Anal. Machine Intell. PAMI-8 (4), 472–481.

Laine, A., Fan, J., 1993. Texture classification by wavelet packet signatures. IEEE Trans. Pattern Anal. Machine Intell. 15 (11), 1186–1191.

Mallat, S., 1989. A theory for multiresolution signal decomposition: The wavelet representation. IEEE Trans. Pattern Recognition Machine Intell. 11 (7), 674–693.

Manthalkar, R., Biswas, P.K., Chatterji, B.N., 2003a. Rotation invariant texture classification using even symmetric Gabor filters. Pattern Recognition Lett. 24 (12), 2061–2068.

Manthalkar, R., Biswas, P.K., Chatterji, B.N., 2003b. Rotation and scale invariant texture features using discrete wavelet packet transform. Pattern Recognition Lett. 24 (14), 2455–2462.

Pichler, O., Teuner, A., Hosticka, B.J., 1996. A comparison of texture feature-extraction using adaptive gabor filtering, pyramidal and tree-structured wavelet transforms. Pattern Recognition 29 (5), 733–742.

Pun, C.M., Lee, M.C., 2001. Rotation-invariant texture classification using a two-stage wavelet packet feature approach. VISP 148 (6), 422–428.

Raghu, P.P., Yegnanarayana, B., 1996. Segmentation of Gabor-filtered textures using deterministic relaxation. IEEE Trans. Image Process. 5 (12), 1625–1636.

Sklansky, J., 1978. Image segmentation and feature extraction. IEEE Trans. Syst. Man Cybernet. 8 (4), 237–247.

Teuner, A., Pichler, O., Hosticka, B.J., 1995. Unsupervised texture segmentation of images using tuned matched Gabor filters. IEEE Trans. Image Process. 4 (6), 863–870.

Tuner, M.R., 1986. Texture discrimination by Gabor functions. Biol. Cyber. 55, 71–82.

Unser, M., 1995. Texture classification and segmentation using wavelet frames. IEEE Trans. Image Process. 4, 1549–1560.

Unser, M., 1986. Local linear transforms for texture measurements. Signal Process. 11, 61–79.

Van De Wouwer, G., Scheunders, P., Van Dyck, D., 1999. Statistical texture characterization from discrete wavelet representations. IEEE Trans. Image Process. 8 (4), 592–598.

Wang, J.W., Chen, C.H., Chien, W.M., Tsai, C.M., 1998. Texture classification using non-separable two-dimensional wavelets. Pattern Recognition Lett. 19 (13), 1225–1234.

Wang, L., Liu, J., 1999. Texture classification using multi resolution Markov random field models. Pattern Recognition Lett. 20 (2), 171–182.

Zhang, D.S., Wong, A., Indrawan, M., Lu, G., 2000. Content based image retrieval using Gabor texture features. In: Proc. of 1st IEEE Pacific Rim Conference on Multimedia (PCM'00), pp. 392–395.

Zhang, J., Tan, T., 2002. Rotation invariant texture segmentation via circular Gabor filters. In: Proc. IEEE International Conference on Pattern Recognition, Quebec City, QC, Canada.

Zhu, Z., Tang, M., Lu, H., 2004. A new robust circular Gabor based object matching by using weighted Hausdorff distance. Pattern Recognition Lett. 25 (4), 515–523.